nature materials

LETTERS

Persistence of magnetic excitations in $La_{2-x}Sr_xCuO_4$ from the undoped insulator to the heavily overdoped non-superconducting metal

M. P. M. Dean[1]★, G. Dellea[2], R. S. Springell[3], F. Yakhou-Harris[4], K. Kummer[4], N. B. Brookes[4], X. Liu[1,5], Y-J. Sun[1,5], J. Strle[1,6], T. Schmitt[7], L. Braicovich[2,8], G. Ghiringhelli[2,8], I. Božović[1] and J. P. Hill[1]★

One of the most intensely studied scenarios of high-temperature superconductivity (HTS) postulates pairing by exchange of magnetic excitations[1]. Indeed, such excitations have been observed up to optimal doping in the cuprates[2–7]. In the heavily overdoped regime, neutron scattering measurements indicate that magnetic excitations have effectively disappeared[8–10], and this has been argued to cause the demise of HTS with overdoping[1,8,10]. Here we use resonant inelastic X-ray scattering, which is sensitive to complementary parts of reciprocal space, to measure the evolution of the magnetic excitations in $La_{2-x}Sr_xCuO_4$ across the entire phase diagram, from a strongly correlated insulator ($x = 0$) to a non-superconducting metal ($x = 0.40$). For $x = 0$, well-defined magnon excitations are observed[11]. These magnons broaden with doping, but they persist with a similar dispersion and comparable intensity all the way to the non-superconducting, heavily overdoped metallic phase. The destruction of HTS with overdoping is therefore caused neither by the general disappearance nor by the overall softening of magnetic excitations. Other factors, such as the redistribution of spectral weight, must be considered.

The undoped high-T_c cuprates such as La_2CuO_4 are antiferromagnetic (Néel-ordered) insulators, with magnetic Bragg peaks and well-defined high-energy magnetic excitations termed magnons[11]. As shown in Fig. 1a, doping rapidly destroys the Néel ordering, leading to the emergence of the pseudogap state and superconductivity. In the underdoped and optimally doped cuprates, superconductivity is accompanied by an 'hour-glass'-shaped dispersion of magnetic excitations around the scattering vector $\mathbf{Q}_{\mathrm{AFM}} = (0.5, 0.5)$ in Fig. 1b (refs 2–6,12). In the lightly overdoped, but still superconducting regime, high-energy magnetic excitations have been observed in $La_{1.78}Sr_{0.22}CuO_4$ (ref. 13) and $YBa_2Cu_3O_7$ (ref. 7). Far less work has been done on the magnetic excitations in the heavily overdoped region of the phase diagram. Neutron scattering studies of $La_{1.70}Sr_{0.30}CuO_4$ report that the **Q**-integrated magnetic dynamic structure factor $S(\omega)$ is much reduced by $x = 0.25$ and that magnetic excitations have effectively disappeared by $x = 0.30$ (ref. 9), where x is the doping level. This observation has been used in support of proposals that spin fluctuations mediate the electron pairing in high-T_c superconductors[1]. A necessary, although not sufficient, condition for such scenarios is that spin fluctuations persist across the superconducting portion of the phase diagram while retaining appreciable spectral weight. For this reason it was suggested that the destruction of HTS in the overdoped cuprates is due to the disappearance of magnetic excitations[8].

Resonant inelastic X-ray scattering (RIXS) at the Cu L_3 edge has recently emerged as a new experimental method for measuring magnetic excitations in the cuprates[7,14–19]. RIXS is particularly well suited to measuring high-energy magnetic excitations and requires only very small sample volumes[14,15]. As explained in ref. 7, this sets it apart from current neutron scattering experiments, which require large single crystals of several cm^3 in volume that are usually very difficult to synthesize, especially in the heavily overdoped region. We also note that Cu L_3 edge RIXS experiments focus on a complementary region of the Brillouin zone in Fig. 1b compared to most **Q**-resolved neutron scattering experiments[20]. RIXS typically measures from $(0, 0)$ towards $(0.5, 0)$; whereas neutron scattering experiments focus around $(0.5, 0.5)$, where the magnetic excitations are strongest. In the absence of a universally accepted, quantitative theory of high-T_c superconductivity, it is essential to consider the excitation spectrum over the whole Brillouin zone.

We synthesized $La_{2-x}Sr_xCuO_4$ films with $x = 0$, 0.11, 0.16, 0.26 and 0.40 using molecular beam epitaxy. These films, unlike bulk samples, have atomically smooth surfaces (root mean square roughness, as measured by atomic force microscopy, down to a few Å), which reduce the diffuse elastic scattering contribution to the spectra[20]. We chose the doping levels to span the $La_{2-x}Sr_xCuO_4$ phase diagram, as indicated by the solid black squares in Fig. 1a.

RIXS spectra for these samples are shown in Fig. 1c. The most intense feature corresponds to optically forbidden *dd* orbital excitations in which the valence band hole, primarily of Cu $d_{x^2-y^2}$ character, is promoted into higher energy orbitals[21]. The intensity of these excitations can provide a reference to compare different RIXS spectra[22]. In the mid-infrared energy scale (50–500 meV) single spin-flip excitations can be excited owing to the spin–orbit coupling of the Cu $2p_{3/2}$ core hole[23,24]. A broad, flat background of intensity arises from charge-transfer excitations of the Cu $d_{x^2-y^2}$ hole into the O $2p$ states. As x increases the *dd* excitations are seen to broaden,

---

[1]Department of Condensed Matter Physics and Materials Science, Brookhaven National Laboratory, Upton, New York 11973, USA, [2]Dipartimento di Fisica, Politecnico di Milano, Piazza Leonardo da Vinci 32, I-20133 Milano, Italy, [3]Royal Commission for the Exhibition of 1851 Research Fellow, Interface Analysis Centre, University of Bristol, Bristol BS2 8BS, UK, [4]European Synchrotron Radiation Facility (ESRF), BP 220, F-38043 Grenoble Cedex, France, [5]Beijing National Laboratory for Condensed Matter Physics, and Institute of Physics, Chinese Academy of Sciences, Beijing 100190, China, [6]Department for Complex Matter, Jožef Stefan Institute, Jamova 39, 1000 Ljubljana, Slovenia, [7]Swiss Light Source, Paul Scherrer Institut, CH-5232 Villigen PSI, Switzerland, [8]CNR-SPIN, Consorzio Nazionale Interuniversitario per le Scienze Fisiche della Materia, Italy. *e-mail: mdean@bnl.gov; hill@bnl.gov

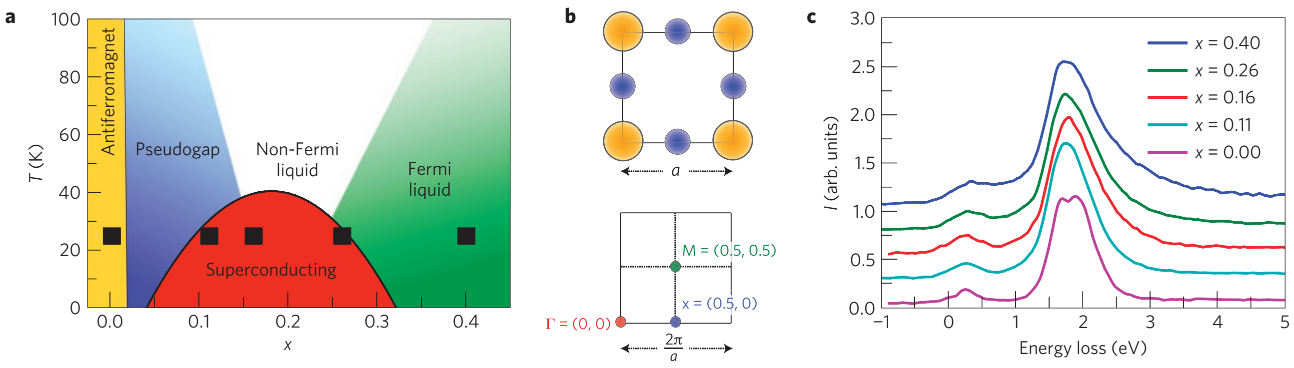

Figure 1 | $La_{2-x}Sr_xCuO_4$ diagrams and RIXS spectra. a, A schematic phase diagram for $La_{2-x}Sr_xCuO_4$ as a function of x. The black lines defining the superconducting and antiferromagnetic states are based on data from ref. 32. The doping levels of the samples studied here, and the temperature at which the measurements were made, are marked by black squares. **b**, Top, the basic structural unit of the cuprates: a CuO_2 plaquette with Cu atoms in orange and O atoms in blue with a lattice spacing of $a \approx 3.8$ Å. Bottom, the reciprocal lattice with high-symmetry points marked and labelled in reciprocal lattice units (r.l.u.). **c**, The RIXS spectrum of $La_{2-x}Sr_xCuO_4$ for different doping levels at $\mathbf{Q} = (0.36, 0)$. The peaks in the 1–3 eV energy window are the *dd* excitations, whereas the low-energy peak around 300 meV arises from magnetic scattering.

indicative of hybridization between the d orbitals and the itinerant states of doped holes. This leads to a tail of intensity extending down into the mid-infrared energy region.

RIXS spectra were measured on all samples from $\mathbf{Q} = (0, 0)$ to $\mathbf{Q} = (0.4, 0)$ (that is, up to 80% of the Brillouin zone boundary) and are plotted in Fig. 2. At $\mathbf{Q} = (0, 0)$ strong specular elastic scattering dominates the spectrum. At higher **Q** we observe a peak on the energy scale of 300 meV. For the undoped ($x = 0$) case this peak corresponds to a magnon[15,16,22], as observed previously by neutron scattering[11]. Examining the spectra at higher doping levels shows the central result of this paper: that this magnon smoothly broadens with doping and persists as a paramagnon right across the $La_{2-x}Sr_xCuO_4$ phase diagram and into the heavily overdoped metallic region. Understanding this observation and how it might relate to HTS is the main challenge posed by our data.

We fit the spectra with a resolution-limited Gaussian to account for the elastic scattering and an anti-symmetrized Lorentzian to account for the magnetic scattering, together with a smooth background (see Supplementary Information for more details). For the $x = 0$ sample, the magnon is well defined in energy[11] and the peak broadening arises primarily from contributions from phonons and multimagnon excitations. This leads to a roughly **Q**-independent broadening of the peak[7]. Figure 3 summarizes the fitting results. Within the scatter of the data points, which is about $\sim$70 meV (or $\sim$20% of the zone boundary energy), the dispersion of the magnetic excitations in Fig. 3a is unchanged. In contrast, the width of the excitations in Fig. 3b increases dramatically with doping. This damping of the magnon with doping is probably due to the magnetic excitations coupling with, and decaying into, Stoner quasiparticles as low-energy electronic states become available.

Measurements spanning the underdoped to slightly overdoped regions of the phase diagram in neodymium[7] yttrium[7] (YBCO) and bismuth[17] based cuprates show comparable widths to our optimally doped $La_{1.84}Sr_{0.16}CuO_4$ (LSCO) sample. Our experiments go beyond optimal doping, as do recent results on Tl-based cuprates[25], and show that the width continues to increase as more electronic states become available for scattering. The similar widths of optimally doped LSCO, YBCO and bismuth are interesting in light of the fact that LSCO is often regarded as more disordered than YBCO (ref. 26). This may imply that the width is primarily determined by the hole concentration level rather than the structural disorder induced by doping.

We also examined the RIXS intensities as a function of doping. As discussed in the Supplementary Information, instrumental instabilities can make measuring RIXS excitations in absolute units challenging[22]. For this reason, we present the **Q**-averaged integrated intensity of the paramagnon in Fig. 3c. Remarkably, the paramagnon is seen to have comparable RIXS intensity across the entire phase diagram, right into the heavily overdoped region.

These results heavily constrain any theoretical description of the magnetism in the cuprates, as this must explain how the magnetic excitations evolve with doping. Motivated by the local moment physics in La_2CuO_4, and possible electronic phase separation in the underdoped cuprates, much theoretical work has described magnetism in the cuprates in terms of residual local moments that exist in the charge-poor region of the lattice[27]. The effect of doping is then primarily to reduce the number of local moments present. In the heavily overdoped region of the phase diagram, such phase separation seems unlikely to be energetically favourable as there is a large kinetic energy cost to localizing the electrons. Despite this, our data show that the local moment-based magnon excitations evolve smoothly and continuously across the phase diagram, into the region where renormalized itinerant quasiparticles have been suggested as explanations for the magnetic response of the cuprates[28]. In particular, our results demonstrate that the heavily overdoped region of the phase diagram retains magnetic correlations and is not a simple non-magnetic Fermi liquid.

It is important to note that we report excitations from $(0.18, 0)$ to $(0.40, 0)$. Inelastic neutron scattering experiments, on the other hand, are predominantly sensitive to the higher intensity excitations around $\mathbf{Q}_{\mathrm{AFM}} = (0.5, 0.5)$, where studies of heavily overdoped cuprates report a strong reduction in the energy and spectral weight of the magnetic excitations[9,10]. In the region of **Q**-space studied here, the intensity of the magnetic excitations are below the signal-to-noise ratio of current **Q**-resolved neutron scattering experiments on doped cuprates. Thus RIXS allows us to measure magnetic excitations in a complementary region of the Brillouin zone. Although in Néel ordered La_2CuO_4 the energy dispersion is symmetric on reflection in the antiferromagnetic Brillouin zone boundary, the same need not be true for $x \gtrsim 0.03$. Furthermore, the intensities differ substantially, depending on whether **Q** is near $(0, 0)$ or $\mathbf{Q}_{\mathrm{AFM}} = (0.5, 0.5)$. Taken together, the RIXS and neutron data imply that doping does not uniformly reduce the intensity of the magnetic excitations. Rather, the excitations around $(0.18 \rightarrow 0.40, 0)$ remain relatively unchanged in integrated intensity whereas the absolute intensity of the excitations around $\mathbf{Q}_{\mathrm{AFM}}$ (which provide most of the total spectral weight) are strongly attenuated. The energy dispersion of the magnetic excitations along $(0.18 \rightarrow 0.40, 0)$ also remains constant as as function of doping, whereas the dispersion near $\mathbf{Q}_{\mathrm{AFM}}$, is strongly renormalized to form the 'hour-glass' feature[2–6,12].

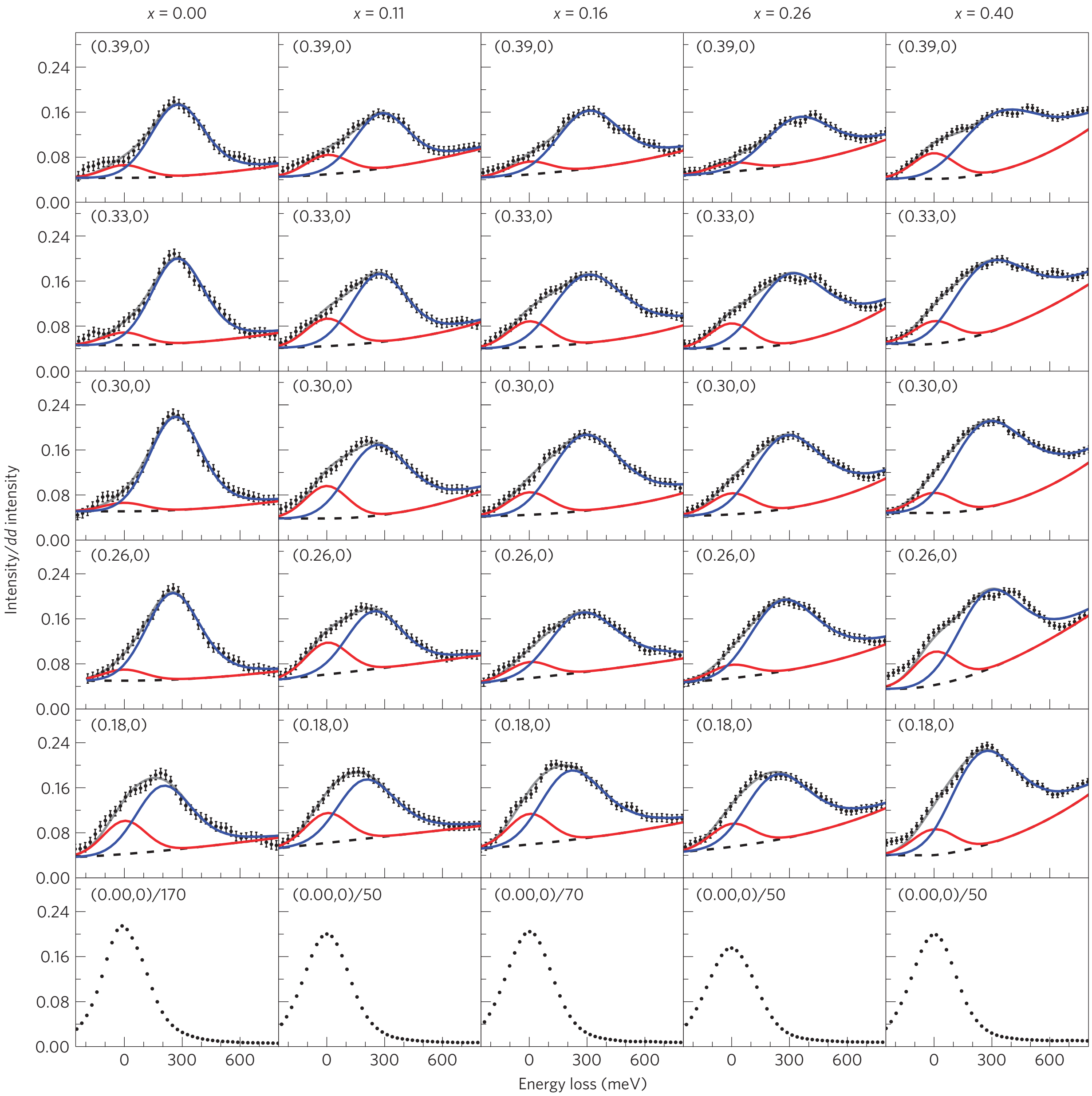

Figure 2 | $La_{2-x}Sr_xCuO_4$ magnetic excitation spectra. The dispersion of the magnetic excitations in $La_{2-x}Sr_xCuO_4$ as function of **Q** and *x*. The filled black circles represent the data and the solid grey line shows the results of the fitting, which is the sum of an elastic scattering contribution (red), an anti-symmetrized Lorentzian capturing the magnetic scattering (blue), and the background (dashed black). The fit was convolved with the experimental resolution—see the Supplementary Information for full details. At $\mathbf{Q} = (0, 0)$ magnetic excitations cannot be observed owing to the very strong elastic specular scattering, and the peak shape primarily reflects the experimental resolution function. The intensities are presented, normalized to the spectral weight in the 1–3 eV region containing the *dd* excitations. The spectra at $\mathbf{Q} = (0, 0)$ have been divided by the factors written on the plot to make them visible on the same scale. Error bars indicate the magnitude of the statistical variations in the summed spectra.

The intensity of the magnetic excitations in undoped La_2CuO_4 is well known from inelastic neutron scattering and has been shown to be reasonably well captured by spin wave theory[11,29]. We recalculated this excitation spectrum using the methods and parameters described in ref. 11. We find that 27% of the total inelastic magnetic intensity lies in the region of the Brillouin zone accessible to RIXS, which was taken to be a circle of radius 0.4 in relative lattice units about $(0, 0)$ (Supplementary Information). It will be very important for future studies to measure whether the magnetic excitations along $(0, 0) \rightarrow (0.25, 0.25)$ scale in a similar way to the excitations along $(0, 0) \rightarrow (0.4, 0)$. However, if we assume this to be the case, our results imply that this 27% of the inelastic magnetic intensity persists with doping, indicating substantial magnetic correlations in the heavily overdosed sample. Furthermore, given that the excitations at $(0.5, 0.5)$ become weaker with doping, the excitations studied here with RIXS will represent a larger fraction of the total scattering weight at optimal doping.

Our results seem to be consistent with the description of magnetic properties of the cuprates across the phase diagram based on the single-band two-dimensional Hubbard model. Numerical studies of this model[30] indeed qualitatively capture both the suppression of intensity around $\mathbf{Q}_{\mathrm{AFM}}$ and the approximate conservation of intensity around $\mathbf{Q} = (0.18 \rightarrow 0.40, 0)$.

The cuprate phase diagram (Fig. 1a) shows a dome-like dependence of T_c as a function of x. On the underdoped $(x < 0.16)$

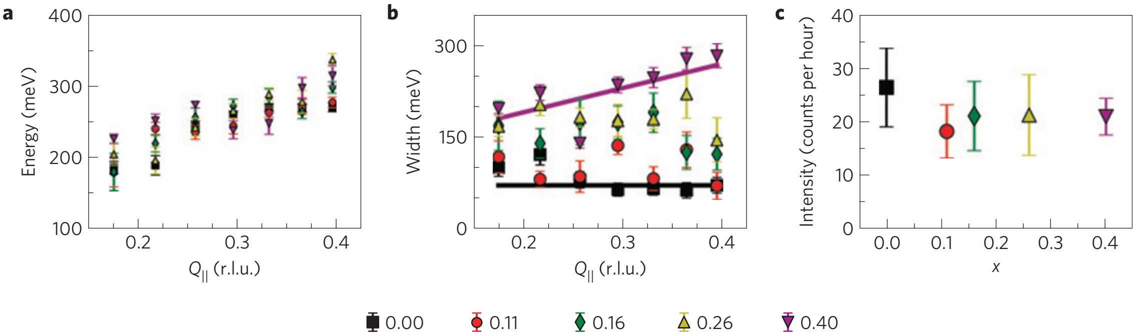

Figure 3 | Evolution with doping of the magnetic excitations in $La_{2-x}Sr_xCuO_4$. **a**, Energy dispersion of the magnetic excitations along $\mathbf{Q} = (Q_{\parallel}, 0)$, showing that the magnetic excitation energy does not change significantly with x. **b**, The $Q_{\parallel}$ dependence of the half-width at half-maximum (HWHM) of the magnetic excitations. The black and purple lines are guides to the eye for the $x = 0$ and $x = 0.40$ data respectively, emphasizing the overall increase of width with x. **c**, The RIXS intensity of the magnetic excitations averaged over the measured **Q** show that, within errors, the intensity of the magnetic excitations is conserved with increasing x. The error bars in **a**,**b** represent the uncertainty in the least-squares fitting routines, whereas in **c** these are combined with an uncertainty due to the instrumental instability (see the Supplementary Information for more details).

side of the phase diagram the drop in T_c and the eventual disappearance of HTS is probably due to the reduction in the density of mobile charge carriers. The reduction in T_c on the overdoped ($x > 0.16$) side, in the face of the increase in the conductivity and the density of itinerant carriers, is probably driven by a reduction in the strength of the pairing interaction. Our results show that the demise of HTS in the overdoped cuprates is not due to changes in the high-energy magnetic excitations, as these remain approximately constant as a function of x. The change in T_c must, therefore, be driven by other factors. These could include the influence of the low-energy magnetic excitations, which are known to change dramatically in the overdoped cuprates. It is also conceivable that factors not captured within the simple Hubbard model may be at play.

Methods

Sample preparation. The $La_{2-x}Sr_xCuO_4$ films were synthesized by atomic layer-by-layer molecular beam epitaxy[31]. We used single-crystal $LaSrAlO_4$ substrates polished with the surface perpendicular to the c-axis, that is, the [001] crystallographic direction. During film deposition, the substrates were kept at $T_s \approx 680\,^{\circ}\mathrm{C}$ under an ozone partial pressure $p = 5 \times 10^{-6}$ torr. The $x = 0$, $x = 0.16$ and $x = 0.40$ films were 40 unit cells (53 nm) thick and the $x = 0.11$ and $x = 0.26$ films were 75 units cells (99 nm) thick. Reflection high-energy electron diffraction was monitored in real time to ensure that the films were atomically smooth and without any secondary-phase precipitates, which was verified *ex situ* by atomic force microscopy. The undoped ($x = 0$) and underdoped ($x = 0.11$) films were annealed under vacuum (2×10^{-8} torr) for one hour to drive out any excess (interstitial) oxygen. X-ray diffraction confirmed high crystalline order and absence of any secondary phases. To evaluate superconducting properties, magnetic susceptibility measurements were performed using the mutual inductance technique. Sharp superconducting transitions were observed in the films with $x = 0.11$ (underdoped, $T_c = 29$ K), 0.16 (optimally doped, $T_c = 39$ K) and 0.26 (overdoped, $T_c = 22$ K); in contrast, the undoped ($x = 0$) and heavily overdoped ($x = 0.40$) films showed no signs of superconductivity. More details are given in the Supplementary Information.

RIXS measurements. RIXS experiments were performed using the AXES instrument at the ID08 beamline at the European Synchrotron Radiation Facility. The spectra were typically collected for 1–2 h, during which time the CCD camera was read out every 5 min. The incident X-ray energy was set to the peak in the measured Cu L_3 edge X-ray absorption spectrum. The X-rays were incident at an angle θ_i with respect to the sample surface and scattered through $2\theta = 130^{\circ}$ in the horizontal scattering plane (see the diagram in the Supplementary Information). We denote the in-plane scattering vector **Q** in reciprocal lattice units (r.l.u.) using the 2D cuprate unit cell shown in Fig. 1b with $a = b = 3.78$ Å. To scan **Q** we varied θ_i by rotating the sample about the vertical axis, thus varying the projection of **Q** into the a^*b^*-plane, where a^* and b^* are the reciprocal lattice vectors. Data reported here used π polarized X-rays, with high-**Q** corresponding to X-rays that leave the sample at grazing angles. The combined resolution function of the monochromator and spectrometer is approximately Gaussian with a HWHM of 130 meV, as determined by measuring the non-resonant elastic scattering from disordered carbon tape. All data were collected at $T = 25(5)$ K.

Received 6 March 2013; accepted 26 June 2013; published online 4 August 2013

References

1. Scalapino, D. J. A common thread: The pairing interaction for unconventional superconductors. *Rev. Mod. Phys.* **84,** 1383–1417 (2012).
2. Bourges, P. *et al.* The spin excitation spectrum in superconducting $YBa_2Cu_3O_{6.85}$. *Science* **288,** 1234–1237 (2000).
3. Tranquada, J. M. *et al.* Quantum magnetic excitations from stripes in copper oxide superconductors. *Nature* **429,** 534–538 (2004).
4. Hayden, S. M., Mook, H. A., Dai, P., Perring, T. G. & Dogan, F. The structure of the high-energy spin excitations in a high-transition-temperature superconductor. *Nature* **429,** 531–534 (2004).
5. Vignolle, B. *et al.* Two energy scales in the spin excitations of the high-temperature superconductor $La_{2-x}Sr_xCuO_4$. *Nature Phys.* **3,** 163–167 (2007).
6. Xu, G. *et al.* Testing the itinerancy of spin dynamics in superconducting $Bi_2Sr_2CaCu_2O_{8+\delta}$. *Nature Phys.* **5,** 642–646 (2009).
7. Le Tacon, M. *et al.* Intense paramagnon excitations in a large family of high-temperature superconductors. *Nature Phys.* **7,** 725–730 (2011).
8. Wakimoto, S. *et al.* Direct relation between the low-energy spin excitations and superconductivity of overdoped high-T_c superconductors. *Phys. Rev. Lett.* **92,** 217004 (2004).
9. Wakimoto, S. *et al.* Disappearance of antiferromagnetic spin excitations in overdoped $La_{2-x}Sr_xCuO_4$. *Phys. Rev. Lett.* **98,** 247003 (2007).
10. Fujita, M. *et al.* Progress in neutron scattering studies of spin excitations in high-T_c cuprates. *J. Phys. Soc. Jpn* **81,** 011007 (2012).
11. Coldea, R. *et al.* Spin waves and electronic interactions in La_2CuO_4. *Phys. Rev. Lett.* **86,** 5377–5380 (2001).
12. Arai, M. *et al.* Incommensurate spin dynamics of underdoped superconductor $YBa_2Cu_3O_{6.7}$. *Phys. Rev. Lett.* **83,** 608–611 (1999).
13. Lipscombe, O. J., Hayden, S. M., Vignolle, B., McMorrow, D. F. & Perring, T. G. Persistence of high-frequency spin fluctuations in overdoped superconducting $La_{2-x}Sr_xCuO_4$ ($x = 0.22$). *Phys. Rev. Lett.* **99,** 067002 (2007).
14. Braicovich, L. *et al.* Dispersion of magnetic excitations in the cuprate La_2CuO_4 and $CaCuO_2$ compounds measured using resonant x-ray scattering. *Phys. Rev. Lett.* **102,** 167401 (2009).
15. Braicovich, L. *et al.* Magnetic excitations and phase separation in the underdoped $La_{2-x}Sr_xCuO_4$ superconductor measured by resonant inelastic x-ray scattering. *Phys. Rev. Lett.* **104,** 077002 (2010).
16. Dean, M. P. M. *et al.* Spin excitations in a single La_2CuO_4 layer. *Nature Mater.* **11,** 850–584 (2012).
17. Dean, M. P. M. *et al.* High-energy magnetic excitations in the cuprate superconductor $Bi_2Sr_2CaCu_2O_{8+\delta}$: Towards a unified description of its electronic and magnetic degrees of freedom. *Phys. Rev. Lett.* **110,** 147001 (2013).
18. Dean, M. P. M. *et al.* Magnetic excitations in stripe-ordered $La_{1.875}Ba_{0.125}CuO_4$ studied using resonant inelastic x-ray scattering. *Phys. Rev. B* **88,** 020403(R) (2013).
19. Zhou, K-J. *et al.* Persistent high-energy spin excitations in iron-pnictide superconductors. *Nature Commun.* **4,** 1470 (2013).
20. Ament, L. J. P., van Veenendaal, M., Devereaux, T. P., Hill, J. P. & Van den Brink, J. Resonant inelastic x-ray scattering studies of elementary excitations. *Rev. Mod. Phys.* **83,** 705–767 (2011).

21. Ghiringhelli, G. *et al.* Low energy electronic excitations in the layered cuprates studied by copper L_3 resonant inelastic x-ray scattering. *Phys. Rev. Lett.* **92,** 117406 (2004).
22. Braicovich, L. *et al.* Momentum and polarization dependence of single-magnon spectral weight for Cu L_3-edge resonant inelastic x-ray scattering from layered cuprates. *Phys. Rev. B* **81,** 174533 (2010).
23. Ament, L. J. P., Ghiringhelli, G., Moretti Sala, M., Braicovich, L. & Van den Brink, J. Theoretical demonstration of how the dispersion of magnetic excitations in cuprate compounds can be determined using resonant inelastic x-ray scattering. *Phys. Rev. Lett.* **103,** 117003 (2009).
24. Haverkort, M. W. Theory of resonant inelastic x-ray scattering by collective magnetic excitations. *Phys. Rev. Lett.* **105,** 167404 (2010).
25. Le Tacon, M. *et al.* Dispersive spin excitations in highly overdoped cuprates revealed by resonant inelastic x-ray scattering. *Phys. Rev. B* **88,** 020501(R) (2013).
26. Alloul, H., Bobroff, J., Gabay, M. & Hirschfeld, P. J. Defects in correlated metals and superconductors. *Rev. Mod. Phys.* **81,** 45–108 (2009).
27. Vojta, M. Lattice symmetry breaking in cuprate superconductors: Stripes, nematics, and superconductivity. *Adv. Phys.* **58,** 699–820 (2009).
28. Brinckmann, J. & Lee, P. A. Renormalized mean-field theory of neutron scattering in cuprate superconductors. *Phys. Rev. B* **65,** 014502 (2001).
29. Headings, N. S., Hayden, S. M., Coldea, R. & Perring, T. G. Anomalous high-energy spin excitations in the high-T_c superconductor-parent antiferromagnet La_2CuO_4. *Phys. Rev. Lett.* **105,** 247001 (2010).
30. Macridin, A., Jarrell, M., Maier, T. & Scalapino, D. J. High-energy kink in the single-particle spectra of the two-dimensional Hubbard model. *Phys. Rev. Lett.* **99,** 237001 (2007).
31. Božović, I. Atomic-layer engineering of superconducting oxides: Yesterday, today, tomorrow. *IEEE Trans. Appl. Supercond.* **11,** 2686–2695 (2001).
32. Keimer, B. *et al.* Magnetic excitations in pure, lightly doped, and weakly metallic La_2CuO_4. *Phys. Rev. B* **46,** 14034–14053 (1992).

Acknowledgements

M.P.M.D. and J.P.H. are supported by the Center for Emergent Superconductivity, an Energy Frontier Research Center funded by the US DOE, Office of Basic Energy Sciences. Work at Brookhaven National Laboratory was supported by the Office of Basic Energy Sciences, Division of Materials Science and Engineering, US Department of Energy under Award No. DEAC02-98CH10886. This work was also partially supported by the Italian Ministry of Research MIUR (Grant No. PRIN- 20094W2LAY). The experiment was performed using the AXES instrument at ID08 at the European Synchrotron Radiation Facility. We acknowledge insightful, continuing discussions with A. James, R. Konik and J. Tranquada.

Author contributions

Experiment: M.P.M.D., G.D., G.G., R.S.S., T.S., F.Y-H., K.K., N.B.B. and L.B. Data analysis and interpretation: M.P.M.D., J.P.H. and X.L. Sample growth I.B. Sample characterization: I.B., Y-J.S. and J.S. Project planning: M.P.M.D., J.P.H. and I.B. Paper writing: M.P.M.D., J.P.H. and I.B.

Additional information

Supplementary information is available in the online version of the paper. Reprints and permissions information is available online at www.nature.com/reprints. Correspondence and requests for materials should be addressed to M.P.M.D. or J.P.H.

Competing financial interests

The authors declare no competing financial interests.